PROCEEDINGS OF SCIENCE

Detection of GeV emission from an ultralong gamma-ray burst with the Fermi Large Area Telescope

Yi-Yun Huang,[a,b,*] **Hai-Ming Zhang,**[a,b] **Kai Yan,**[a,b] **Ruo-Yu Liu**[a,b] **and Xiang-Yu Wang**[a,b]

[a] *School of Astronomy and Space Science, Nanjing University, Nanjing 210093, China*
[b] *Key Laboratory of Modern Astronomy and Astrophysics (Nanjing University), Ministry of Education, Nanjing 210093, China*

E-mail: hmzhang@nju.edu.cn, xywang@nju.edu.cn

GRB 220627A, detected by Fermi Gamma-ray Burst Monitor (GBM), is a potential gravitationally lensed gamma-ray burst (GRB), because it has two similar episodes in terms of temporal shapes and spectra. However, by analyzing data from the Fermi Large Area Telescope, we found significant differences in gamma-ray photon numbers between the two episodes. This evidence, combined with a comprehensive spectral study, strongly suggests that GRB 220627A isn't a lensed burst. Instead, it is identified as an ultralong gamma-ray burst, one with emissions lasting over 1000 seconds. Notably, this is the first observation of GeV emissions from such a long burst. Additionally, the detection of a 15.7 GeV photon during the early prompt phase places a lower limit of $\Gamma \geq 300$ on the bulk Lorentz factor of the GRB ejecta. The constraint on the bulk Lorentz factor could shed light on the origin of ultralong GRBs.

38th International Cosmic Ray Conference (ICRC2023)
26 July - 3 August, 2023
Nagoya, Japan

*Speaker

PoS(ICRC2023)828

1. Introduction

Gamma-ray bursts (GRBs) are the most powerful explosive phenomena in the universe. Usually, based on their duration (whether lasting shorter than 2 seconds), they are divided into two classes [11]: short GRBs which are thought to come from the merging of two compact celestial objects [1], and long GRBs which are believed to arise from the massive stars collapsing [6]. Moreover, some works proposed an additional category of 'ultra-long' gamma-ray bursts (ULGRBs) for GRBs lasting longer than 1000 s[10]. Such long duration requires different progenitors to support, such as blue supergiants [14], white dwarf tidal disruption events (WD-TDEs; [9]), and newborn magnetars [7]. However, there is no evidence for each models, all of them can be possible.

At 21:21:00.09 UT on 2022 June 27, the Fermi Gamma-ray Burst Monitor (GBM) triggered and located GRB 220627A [4], which was also detected by the Large Area Telescope (LAT; [3]), Konus-Wind [5], and Swift-BAT-GUANO [15]. Separately, about 1000 s later at 21:36:56.39 UT, the GBM triggered, localized to a similar location, which was regarded as GRB 220627A triggered once again by the GBM. The duration (T_{90}) of the gamma-ray emission in the first episode is about 138 s (10–1000 keV), and that in the second episode is 127 s (10–1000 keV) [16]. Due to the similar temporal shapes and spectra in the two episodes, GRB 220627A is speculated to be a gravitationally lensed GRB [16]. On the other hand, if the emission origin in the second episode is not due to gravitational lensing, GRB 220627A will be an ultralong GRB, given its extremely long duration. In this study, we use both GBM and LAT data to test these scenarios.

2. Data analysis

GBM assembles 12 sodium iodide (NaI) and two bismuth germanate (BGO) scintillation detectors, covering the energy range 8 keV−40 MeV [12]. We only choose three detectors which has the smallest viewing angles with respect to the GRB source direction to analyze for every episode. For the first trigger, we selected two NaI detectors (namely $n0$ and $n3$) and one BGO detector (namely b0) for our analysis, for the second trigger, we selected $n6$, $n7$ and b1 for our analysis. While Fermi-GBM triggered and located GRB 220627A, Fermi-LAT also detected it which at that time was 27° from the LAT boresight. In the second episode, the burst was still within the field of view of LAT with a boresight angle of 56.°8.

In the Fermi-LAT analysis, only the data within a 14° × 14° region of interest (ROI) centered on the position of GRB 220627A are considered. We perform an unbinned maximum likelihood analysis for this GRB, and considering the LAT $TRANSIENT$ events between 100 MeV and 30 GeV. The corresponding instrument response function (IRF) ($P8R3\_TRANSIENT020\_V3$) is used. A maximum zenith angle of 100° is adopted to reduce the contamination from the γ-ray Earth limb. For the main background component, we consider the isotropic emission template ("$iso\_P8R3\_TRANSIENT020\_V3\_v1.txt$") and the diffuse Galactic interstellar emission template (IEM; $gll\_iem\_v07.fits$) in our analysis. The parameters of isotropic emission and IEM are left free. To estimate the significance of the GRB, we use the maximum likelihood test statistic (TS)[1].

[1]TS is defined by TS= $2(\ln \mathcal{L}_1 - \ln \mathcal{L}_0)$, where $\mathcal{L}_1$ and $\mathcal{L}_0$ are maximum likelihood values for the background with the GRB and without the GRB (null hypothesis)

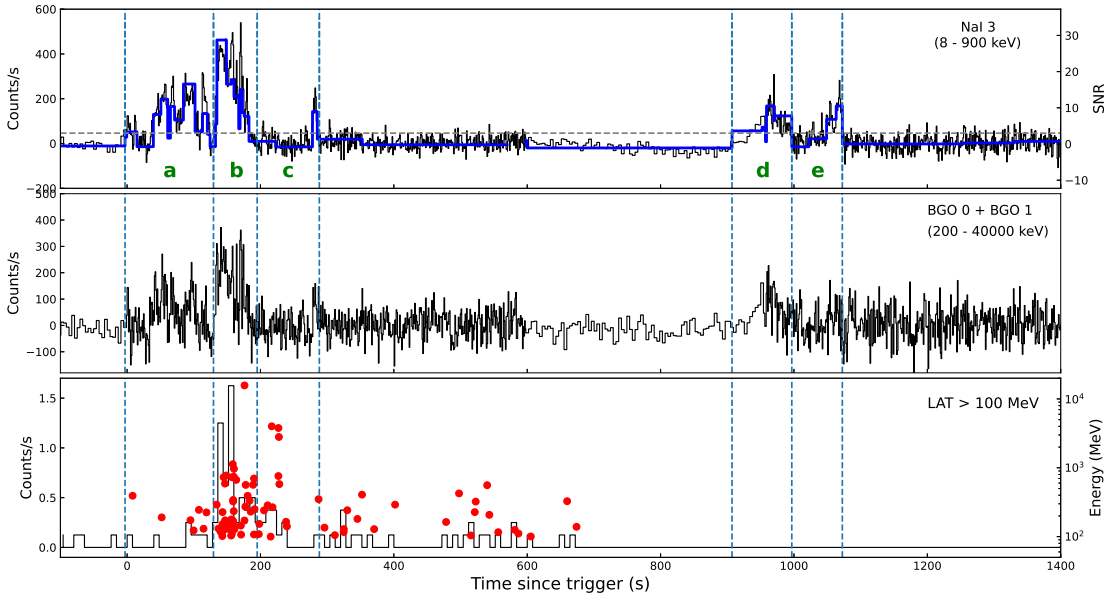

Figure 1: GBM and LAT light curves of GRB 220627A. The background subtracted light curves of NaI and BGO are extracted from the CSPEC type data, which use a 1024 ms time bin after the detector trigger and a 4096 ms time bin before the detector trigger. The blue solid line represents the Bayesian block light curve and the gray dashed line represents that the S/R is equal to 3. The last panel shows the LAT TRANSIENT class events for energies >100 MeV using 10 s time bins. The red points show the arrival time and corresponding energy of LAT photons. The vertical dashed lines indicate the time intervals for the time-resolved spectral analysis derived from the Bayesian block: T_0 +(-3.08, 129.53, 195.07, 288.26, 907.15, 996.75, 1072.53) s.

The TS value for GRB 220627A is found to be 182.89 (corresponds to a detection significance of 13.52σ) in 0–700 s.

In Figure 1, we show the GBM and LAT light curves in several energy bands. To measure the time variability of this GRB, we employ the Bayesian block method [17] on the photon events between 8 and 900 keV, which are indicated by the blue lines in Figure 1. And half of the minimum block size is taken as the minimal variability time $\delta t \simeq 1.79$ s for this burst.

3. Implication for the lensed GRB scenario

Gravitational lensing creates multiple replicas of a source, differing in intensity but maintaining identical spectral shapes. For sources with time variations, the temporal profiles remain consistent but are temporally offset among the different images. Based on this phenomenon, we testify the lensed GRB scenario of GRB 220627A. We firstly perform a joint spectral analysis of the LAT and GBM data across both emission episodes. For each spectrum, we applied the Band function and cutoff power-law (CPL) function to determine the best fit. The formulation for the Band model is

as follows:

$$N(E) = \begin{cases} A(\frac{E}{100\,\mathrm{keV}})^{\alpha}\exp(-\frac{E}{E_c}),\ E < (\alpha-\beta)E_c \\ A\left[\frac{(\alpha-\beta)E_c}{100\,\mathrm{keV}}\right]^{\alpha-\beta}\exp(\beta-\alpha)(\frac{E}{100\,\mathrm{keV}})^{\beta}, E \geq (\alpha-\beta)E_c \end{cases} \quad (1)$$

where α and β are low-energy and high-energy photon spectral indices. The peak energy E_p is related to the cutoff energy, E_c, through $E_p = (2+\alpha)E_c$. The CPL model is expressed as

$$N(E) = AE^{-\lambda}\exp(-E/E_c), \quad (2)$$

where λ is the power-law photon index below the cutoff energy and E_c is e-folding energy. The fit results are summarized in Table 1, and the spectra and residuals are shown in Figure 2 for the best-fit model.

We employed the BIC method to identify the best-fit model.[2] From Table 1, we can find that the best spectrum of the first episode emission follows by a CPL plus an extra hard PL component. The average of photon flux of GRB 220627A in the LAT energy band is $(2.88 \pm 0.47) \times 10^{-5}$ photons cm^{-2} s^{-1} for the first episode. Taking into account the exposure time and effective area of LAT during this period, there were 48.53 ± 7.89 photons above 100 MeV from GRB 220627A. On the other hand, no photons above 100 MeV were detected by LAT in the second episode. The spectrum in GBM band follows by a CPL model. As the lensing scenario described, we hypothesize that the spectral shape of the second episode mirrors that of the first, which also have a same hard component in LAT band. That requires that 5.98 ± 0.97 photons above 100 MeV should have been detected by LAT. The Poisson probabilities of detecting gamma-ray photons with $N < 1$ (N is the total number of photon from the GRB detected by LAT) to be 1.42×10^{-7}, suggesting that the lensing scenario can be ruled out at a confidence level of 5.1σ.

4. Constraints on the bulk Lorentz factor

Since GRB 220627A is an ultra-long GRB, the bulk Lorentz factor (Γ) of the ejecta can help us understand its physics. It is widely believed that the prompt emission arises from ultrarelativistic ejecta, and escape out of the source without suffering from absorption due to pair production ($\gamma\gamma \rightarrow e^+e^-$) [8].To ensure the optical depth for high-energy photons survive under $\tau_{\gamma\gamma} \leq 1$ within the source, we can obtain a lower boundary for the bulk Lorentz factor (Γ) of the emitting region.

For our analysis of GRB 220627A, we adopt a simple one-zone model where the high-energy photons come from the same region as the low-energy target photons, as suggested by a common spike seen in both the LAT and GBM detectors, as shown in Figure 1. For annihilation with photons of energy E_M the target photons should possess energy exceeding $E_t = 2\Gamma^2(m_ec^2)^2/[E_M(1+z)^2]$, where E_M is the maximum energy of the photons detected by LAT and z is the redshift of GRB 220627A. These photons usually come from the high-energy part of the prompt emission spectrum.

[2]BIC is defined as $BIC = \chi^2 + klnN$, where χ^2 is the fit statistic, N is the number of data points, and k is the number of free parameters of the model. The strength of the evidence against the model with the higher BIC value can be summarized as follows [13]. (1) If $\Delta_{\mathrm{BIC}} \geq 2$, there is no evidence against the higher BIC model; (2) if $4 \leq \Delta_{\mathrm{BIC}} \leq 7$, positive evidence against the higher BIC model is given; (3) if $\Delta_{\mathrm{BIC}} \geq 10$, very strong evidence against the higher BIC model is given.

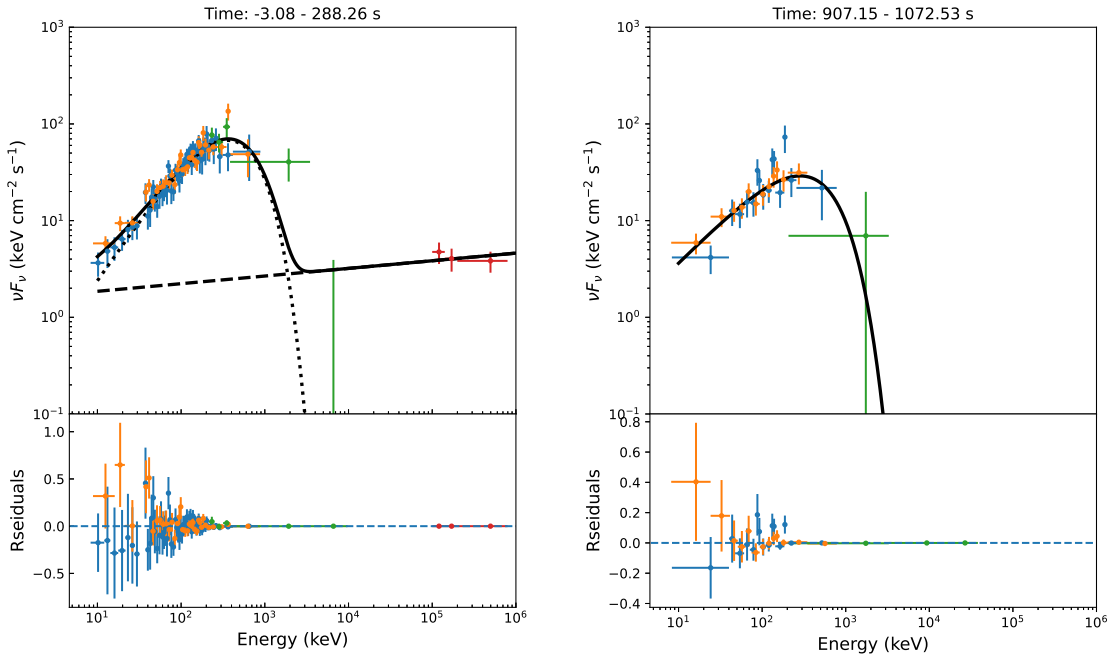

Figure 2: Broadband spectrum of of GRB 220627A in the two emission episodes. Left panel: the time-integrated spectrum measured from $T_0 - 3.08$ s to $T_0 + 288.53$ s and the fitting with the CPL+PL model. The dotted and dashed lines represent the CPL component and the PL component, respectively, and the solid lines represent the sum of them. Right panel: the time-integrated spectrum measured from $T_0 + 907.15$ s to $T_0 + 1072.53$ s and the fitting with the CPL model.

The $\gamma\gamma$ optical depth ($\tau_{\gamma\gamma}$) can be given by [2]

$$\tau_{\gamma\gamma}(E_M) = 2^{1+2\beta} I(\beta) \frac{(-2-\beta)\sigma_{\rm T} L_\gamma (E>E_{\rm peak})\,\delta t\,\Gamma^{2(1+\beta)}}{4\pi R^2 E_{\rm peak}(1+z)} \times \left[\frac{m_e^2 c^4}{E_M E_{\rm peak}(1+z)^2}\right]^{1+\beta} \tag{3}$$

where $\sigma_{\rm T}$ is the Thomson cross section, and β is the high-energy spectral index. The radius of the fireball is given by $R = 2\Gamma^2 c\delta t$ with δt ($\simeq 1.79$ s) being the variability timescale of a single pulse; $I(\beta) = \int_0^1 y g(y) dy/(1-y^2)^{2+\beta}$ with $g(y) = \frac{3}{16}(1-y^2)\left[(3-y^4)\ln\frac{1+y}{1-y} - 2y(2-y^2)\right]$. Here we assume that only photons with energy beyond the spectral $E_{\rm peak}$ are energetic enough to annihilate with high-energy photons, and hence the low-energy spectral slope α does not show up in the expression. The maximum energy of the LAT detected photons in GRB 220627A is $E_M = 15.73$ GeV. From the above equation, we obtain a lower limit on the bulk Lorentz factor of $\Gamma \geq 300$ for GRB 220627A.

5. Summary

In this work, we detect GeV emissions from an exceptionally long-lasting GRB (GRB 220627A) by using Fermi-LAT data. However there is a significant flux ratio difference between GeV and

Table 1: Spectral fitting results of the GBM/LAT emission for the two episodes.

Model	Band	CPL	Band+PL	CPL+PL
Episode I: T_0-3.08–T_0+288.26 s				
Band fuction				
α	-0.89 ± 0.04		-0.88 ± 0.07	
β	-2.45 ± 0.02		-2.45 ± 0.04	
E_p (keV)	334.08 ± 33.32		327.936 ± 58.84	
CPL				
λ		0.91 ± 0.03		0.73 ± 0.10
E_c (keV)		361.43 ± 31.58		286.96 ± 38.00
Powerlaw				
Index			1.92 ± 0.05	1.92 ± 0.05
C-stat/dof	766.06/322	2243.42/323	752.30/320	752.39/321
BIC	789.21	2260.78	787.02	781.32
Episode II: T_0+907.15–T_0+1072.53 s				
Band fuction				
α	1.05 ± 0.05			
β	< -9.27			
E_p (keV)	247.77 ± 66.45			
CPL				
λ		1.06 ± 0.11		
E_c (keV)		248.64 ± 66.58		
Powerlaw				
Index				
C-stat/dof	508.83/340	508.83/341		
BIC	532.19	526.35		

keV/MeV emissions across the two episodes of this GRB. Such a spectral difference challenges the possibility of a lensed GRB interpretation, leading us to determine that GRB 220627A is inherently an ultralong GRB. Meanwhile, A brief spike in the GeV emission corresponds with the keV/MeV emission, indicating both might have an internal origin. The presence of GeV photons also suggests a bulk Lorentz factor of at least $\Gamma \geq 300$ for the emission area, which could offer a vital insight into differentiating between various ULGRB models.

References

[1] Abbott, B. P., Abbott, R., Abbott, T. D., et al. 2017, ApJL, 848, L12, doi: 10.3847/2041-8213/aa91c9

[2] Chen, Y., Liu, R.-Y., & Wang, X.-Y. 2018, MNRAS, 478, 749, doi: 10.1093/mnras/sty1171

[3] di Lalla, N., Axelsson, M., Arimoto, M., Omodei, N., & Crnogoreeviae, M. 2022, GRB Coordinates Network, 32283, 1

[4] Fermi GBM Team. 2022, GRB Coordinates Network, 32278, 1

[5] Frederiks, D., Lysenko, A., Ridnaya, A., et al. 2022, GRB Coordinates Network, 32295, 1

[6] Galama, T. J., Vreeswijk, P. M., van Paradijs, J., et al. 1998, Nature, 395, 670, doi: 10.1038/27150

[7] Gompertz, B., & Fruchter, A. 2017, ApJ, 839, 49, doi: 10.3847/1538-4357/aa6629

[8] Krolik, J. H., & Pier, E. A. 1991, ApJ, 373, 277, doi: 10.1086/170048

[9] Krolik, J. H., & Piran, T. 2011, ApJ, 743, 134, doi: 10.1088/0004-637X/743/2/134

[10] Levan, A. J., Tanvir, N. R., Starling, R. L. C., et al. 2014, ApJ, 781, 13, doi: 10.1088/0004-637X/781/1/13

[11] Mazets, E. P., Golenetskii, S. V., Ilinskii, V. N., et al. 1981, Astrophys. Space Sci., 80, 3, doi: 10.1007/BF00649140

[12] Meegan, C., Lichti, G., Bhat, P. N., et al. 2009, ApJ, 702, 791, doi: 10.1088/0004-637X/702/1/791

[13] Nunes, R. C., Pan, S., Saridakis, E. N., & Abreu, E. M. C. 2017, JCAP, 2017, 005, doi: 10.1088/1475-7516/2017/01/005

[14] Perna, R., Lazzati, D., & Cantiello, M. 2018, ApJ, 859, 48, doi: 10.3847/1538-4357/aabcc1

[15] Raman, G., Tohuvavohu, A., DeLaunay, J., & Kennea, J. A. 2022, GRB Coordinates Network, 32287, 1

[16] Roberts, O. J., Hristov, B., Meegan, C., & Fermi Gamma-ray Burst Monitor Team. 2022, GRB Coordinates Network, 32288, 1

[17] Scargle, J. D., Norris, J. P., Jackson, B., & Chiang, J. 2013, ApJ, 764, 167, doi: 10.1088/0004-637X/764/2/167

PoS(ICRC2023)828